

Hierarchical Assembly of DNA Nanostructures Based on Four-Way Toehold-Mediated Strand Displacement

Tong Lin,^{†,‡} Jun Yan,[†] Luvena L. Ong,^{§,||,#} Joanna Robaszewski,^{§,||} Hoang D. Lu,^{§,△} Yongli Mi,[‡] Peng Yin,^{*,§,⊥} and Bryan Wei^{*,†,⊥}

[†]School of Life Sciences, Tsinghua University-Peking University Center for Life Sciences, Center for Synthetic and Systems Biology, Tsinghua University, Beijing 100084, China

[‡]Department of Chemical and Biological Engineering, The Hong Kong University of Science and Technology, Kowloon, Hong Kong SAR

[§]Wyss Institute for Biologically Inspired Engineering, Harvard University, Boston, Massachusetts 02115, United States

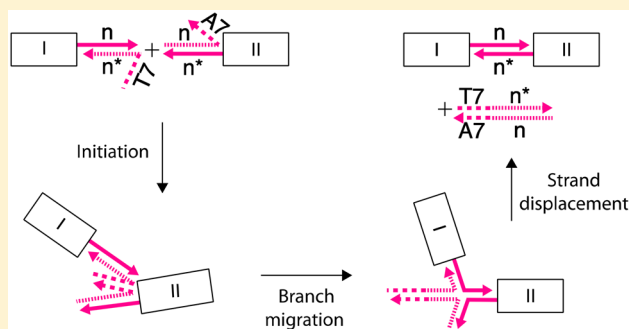
^{||}Harvard-Massachusetts Institute of Technology (MIT) Division of Health Sciences and Technology, MIT, Cambridge, Massachusetts 02139, United States

[⊥]Department of Systems Biology, Harvard Medical School, Boston, Massachusetts 02115, United States

S Supporting Information

ABSTRACT: Because of its attractive cost and yield, hierarchical assembly, in which constituent structures of lower hierarchy share a majority of components, is an appealing approach to scale up DNA self-assembly. A few strategies have already been investigated to combine preformed DNA nanostructures. In this study, we present a new hierarchical assembly method based on four-way toehold-mediated strand displacement to facilitate the combination of preformed DNA structural units. Employing such a method, we have constructed a series of higher-order structures composed of 5, 7, 9, 11, 13, and 15 preformed units respectively.

KEYWORDS: DNA nanotechnology, hierarchical assembly, toehold-mediated strand displacement, single-stranded tiles



Structural DNA nanotechnology has advanced at an extraordinary pace over the past three decades, and increasingly more complex structures have been demonstrated in the field.^{1–20} A major challenge is to scale up self-assembly further to build structures of expanded sizes and higher complexity. There are several approaches to scale up DNA self-assembly. The most straightforward method for origami-based self-assembly is to use a longer scaffold. For example, by adopting 51 kb lambda viral DNA instead of 7 kb M13 viral DNA as the scaffold, the size of the self-assembled origami structure can be multiplied several times over.²¹ However, it could be difficult to get a satisfactory folding quality with a longer scaffold. For a LEGO-based self-assembly approach, increasing the number of building blocks and/or the size of the building blocks gives rise to larger structures^{11–13} but could suffer substantial drop in self-assembly yield. Instead of self-assembly in one pot, larger structures can also be constructed hierarchically. Researchers have implemented different strategies to combine preformed structures (e.g., origami units) into higher order, using either (i) sticky end association,^{14–16,20,22–27} (ii) geometric matching with blunt end stacking,^{28–31} or (iii) the guidance from a scaffold.^{18,32} A number of homo- and heteromultimers have already been

generated from preformed origami units using different combinations of these strategies.

In this study, we demonstrate a new method to assemble preformed DNA nanostructure units made of single-stranded tiles (SSTs) into structures of higher order. Individual units are designed to combine by sticky end association between the matching units. The sticky ends are initially covered by partner protection tiles with toeholds during the formation of individual units. A four-way junction forms upon recognition of the overhanging toeholds.^{33,34} Subsequently, the protection tiles are displaced, and the sticky ends are paired. Multiple toehold-mediated strand displacement events collectively facilitate the association of many pairs of complementary connection tiles, which leads to the combination of the matching structural units. Our implementation based on this scheme results in a series of higher-order structures composed of 5, 7, 9, 11, 13, and 15 preformed SST unit structures (with unit size comparable to a typical origami structure) respectively.

Received: April 5, 2018

Revised: June 20, 2018

Published: July 10, 2018

Results. DNA nanostructures assembled from SSTs are adopted as the basic units for construction of higher-order structures in this study. Multiple units share the same core tiles but vary in connection and protection tiles. A standard Z-shaped core tile is composed of four binding domains, which are complementary to the domains of four neighboring tiles.³⁵ The four consecutive domains of a core tile are 10, 11, 10, and 11 nucleotides (nt) long. A standard connection tile is also composed of four consecutive binding domains (10, 11, 10, and 11 nt), two of which are complementary to domains in core tiles and two of which are complementary to domains in their respective protection tiles (and are ultimately complementary to specific domains in the connection tiles of a matching unit). A protection tile has a binding domain (11 nt) complementary to that of a specific connection tile followed by seven consecutive thymine nucleotides (T7) or seven consecutive adenine nucleotides (A7) (Figure 1 and more

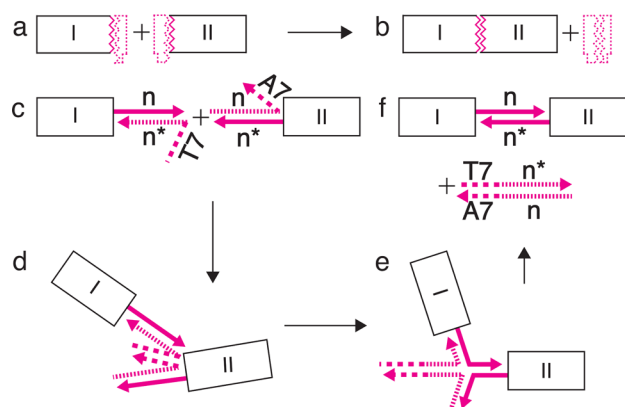


Figure 1. Combination of preformed DNA nanostructures based on four-way toehold-mediated strand displacement. Simplified two-unit assembly is shown in diagrams a and b, with details shown in c–f (only one of many pairs of connection/protection tiles is shown for illustrative purposes; protection tile domains shown in condensed dashed lines and toehold domains in expanded dashed lines). (a) Two preformed units with connection tiles (solid magenta zigzag lines) covered by protection tiles (dashed magenta boxes with overhangs indicating T7 and A7 toeholds) before combination. (b) The combination of the two matching units with paired protection tiles as a byproduct. (c) Before combination, the connection tiles are covered by protection tiles with toeholds. n/n^* indicates the complementary sequences of the protection and connection tiles. (d) Toeholds of T7 and A7 initiate a four-way junction between two matching units. (e) The four-way junction point is mobile along complementary domains of the partner connection tiles. (f) When the branch migration reaches a point of full complementarity between two connection tiles, the paired protection tiles dissociate from the combined units.

details in Figure S1). Besides its role in preventing random aggregation and blunt end stacking,^{11,12} the T7 or A7 segment also serves as a toehold to mediate four-way strand displacement. A typical preformed structural unit as shown in Figure S1 is composed of 350 core DNA strands (322 center Z-shaped tiles and 28 boundary tiles on the top and bottom rows; 25 rows and 14 columns) and 25 connection tiles (12 or 13 in a column on each side of an individual unit; terminal tiles instead of connection tiles are available on a terminal side of a terminal unit), designed specifically to pair up with their counterparts in a matching unit, and 48 protection tiles (24 on

each side, excluding terminal tiles) to cover the corresponding connection tiles.

Because multiple units share core tiles, it is necessary to use hierarchical construction, first forming the individual units and then combining the purified units together. The sticky domains of connection tiles are initially covered by protection tiles before they pair with the desired complementary partners in the successive step (Figure 1, a and b). The T7 toehold of a protection tile from a particular unit binds to the A7 toehold of its partner protection tile from another unit to initiate a four-way junction (Figure 1, c and d). The junction point is mobile, migrating back and forth along complementary domains (depicted as n/n^*) of the partner connection tiles (Figure 1, d and e). When the branch migration reaches a point forming a fully complementary duplex of two matching protection tiles, the newly formed duplex is displaced from their respective units as the two partner connection tiles pair with each other simultaneously (Figure 1f). Multiple strand displacement events along the interface between two matching units collectively result in their final combination.

The details of the seven-unit design and construction (Figure 2 and more details in Figure S2) are given here as an example of our general assembly method. We designed six groups of connection tiles for the left sides (designated nX^*) of the base unit structures, six groups of connection tiles for the right sides (nX), and 12 corresponding groups of protection tiles, pX (left side) and pX^* (right side) ($X \in \{A, B, C, D, E, F\}$). The first (leftmost) unit has paired nA and pA^* groups on its right side. The second unit has paired nA^* and pA groups on its left side and paired nB and pB^* groups on its right side. Similarly, the third unit contains nB^*/pB and nC/pC^* groups, the fourth nC^*/pC and nD/pD^* , the fifth nD^*/pD and nE/pE^* , and the sixth nE^*/pE and nF/pF^* , and finally the left side of the last (rightmost) unit contains the nF/pF^* groups (Figure S2a). For a simpler nomenclature, we name the units by their constituent connection tiles as L-A(T7), A*-B(A7), B*-C(T7), C*-D(A7), D*-E(T7), E*-F(A7), and F*-R(T7) (shown as I, II, III, IV, V, VI, and VII in Figures 2 and S2). L or R denotes the group of terminal tiles on either the leftmost or rightmost terminal side of the assembled strip. T7 or A7 inside the brackets denotes the type of overhang present in the protection tiles. When the seven units are mixed, strand displacement takes place with T7 or A7 overhangs as toeholds. Using units A*-B(A7) and B*-C(T7) as an example reaction, when protection tiles pB^* of unit A*-B(A7) and protection tiles pB of unit B*-C(T7) are displaced, the corresponding connection tiles nB and nB^* associate, and units A*-B(A7) and B*-C(T7) combine as a result (Figure 2b). All seven units are designed to combine by the same mechanism of strand displacement based sticky end association. Different groups of connection/protection tiles can be shuffled as long as individual units are arranged with protection tiles of either T7 or A7 on both ends. For example, an alternative seven-unit arrangement is L-C(T7), C*-F(A7), F*-E(T7), E*-B(A7), B*-A(T7), A*-D(A7), and D*-R(T7).

All component strands for a preformed structural unit were mixed at a nominal concentration without careful adjustment of stoichiometry in $0.5 \times$ TBE supplemented with 15 mM Mg^{2+} . The mixture was subjected to annealing from 90 to 25 °C over 17 h or from 90 to 10 °C over 24 h. Individual preformed units were purified separately from target gel bands after native agarose gel electrophoresis (Figure S3), and the morphology of the purified units was characterized under AFM

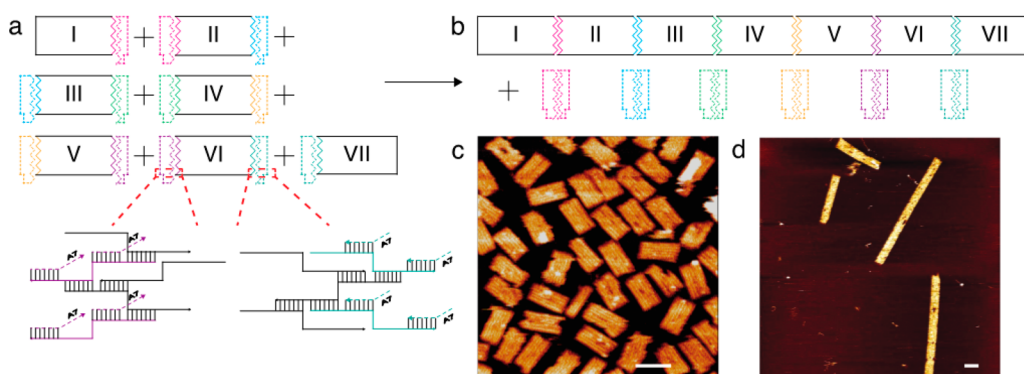


Figure 2. Seven-unit hierarchical assembly. (a and b). Schematic diagrams of seven individual preformed units with connection and protection tiles before (a) and after (b) combination (solid zigzag lines represent connection tiles, and dashed boxes represent protection tiles). A zoomed-in view shows strand-level details of connection/protection tiles of a constituent unit (unit VI). (c) AFM image of an individual unit. (d) AFM image of the strip assembled from seven preformed units. Scale bars: 100 nm.

(Figure 2c). A second round of annealing under isothermal conditions (e.g., 40 °C, Figure S4) for 17 h was performed in $0.5 \times$ TBE supplemented with 15 mM Mg^{2+} to assemble the purified units into the desired multimeric strip. The assembly yield of preformed units without purification was much lower (results not shown), and therefore purified units were prepared for multimerization in this study. According to our optimization on multimerization, more sticky ends between the matching units or units of higher concentration led to a higher combination efficiency (Figures S5 and S6). The preferred denser sticky ends also indicated that the corresponding steric hindrance was limited. The sample collected after the second round of annealing was subjected to AFM imaging. In the case of the seven-unit strip, the desired product with all seven constituent units was observed alongside byproducts with fewer constituent units (Figure 2d). The yield (11%) was calculated by dividing the number of constituent SST units in the seven-unit strips by the number of all identifiable units in several AFM images. Similar two-step hierarchical assembly was performed to form structures with different numbers of preformed units, including 5, 9, 11, 13, and 15 units (yields from 4% to 29%), each with dedicated groups of connection tiles and protection tiles (Figures 3 and S7–S12). When compared with the one-pot 2D assembly from SSTs, the hierarchical assembly method provided a higher yield and a significantly lowered synthesis cost (Tables S1 and S2).

Annealing temperature was optimized so that the association interaction between units was favored, while the integrity of individual units was preserved (Figure S4). According to our experiments with five-unit combination, the formation of the desired product was favored under isothermal annealing temperatures ranging from 36 to 44 °C, while higher temperatures led to incomplete assembly or the total disassociation of structural units. Although strand displacement took place relatively quickly, reactions in this study involved multiple strand displacement events from many units, and an annealing time longer than 12 h was necessary to combine units into a higher order.

To monitor assembly based on toehold-mediated strand displacement, fluorescent labeling was applied, and a time-course assay was performed with a trimeric system of preformed units 1, 2, and 3 (Figures 4 and S13–14). One of the protection tiles of unit 1 was modified with a FAM fluorophore (Figure 4a). When this modified protection tile

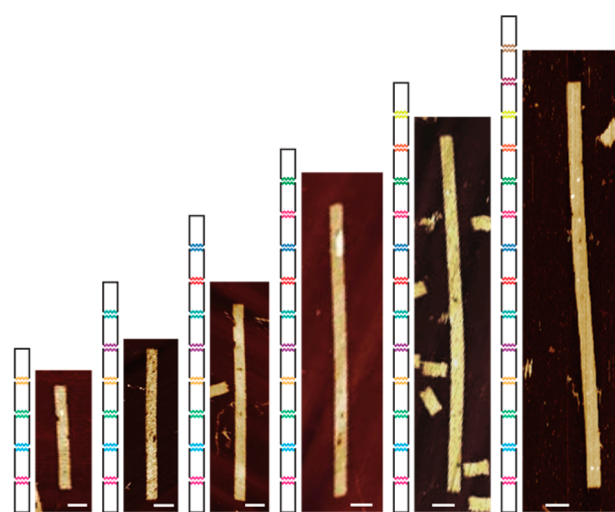


Figure 3. Hierarchical assembly of strips with different numbers of constituent units. From left to right, hierarchical assembly of strips with 5, 7, 9, 11, 13, and 15 units, respectively. Schematic diagrams (left) and AFM images (right) are shown side by side. Scale bars: 100 nm.

met its partner from the matching unit (unit 2), it dissociated from the original unit. Therefore, the disappearance of the fluorescent signal from the unit served as an indicator of successful assembly based on four-way toehold-mediated strand displacement (Figure 4b). As shown in gel electrophoresis (Figure 4c,d, Figure S13) and AFM imaging (Figure S14) results, the desired trimer formed gradually over the 20 h time course. The fluorescent signal from the protection tiles was not recorded on the trimer band because the fluorophore-modified strand detached upon trimerization (Figure S11). In the control group consisting solely of unit 1, the fluorescent protection tile did not fall off of the unit spontaneously, and the FAM signal stayed relatively constant over the entire time course (Figure 4c and Figure S13). Such a constant level of fluorescence indicates that the displacement of the protection tiles is a result of four-way toehold-mediated strand displacement.

Discussion. A widely adopted strategy to combine multiple individual DNA nanostructure units is to directly design units with different sets of complementary connection sequences, as is seen with DNA origami units. Due to random aggregation,

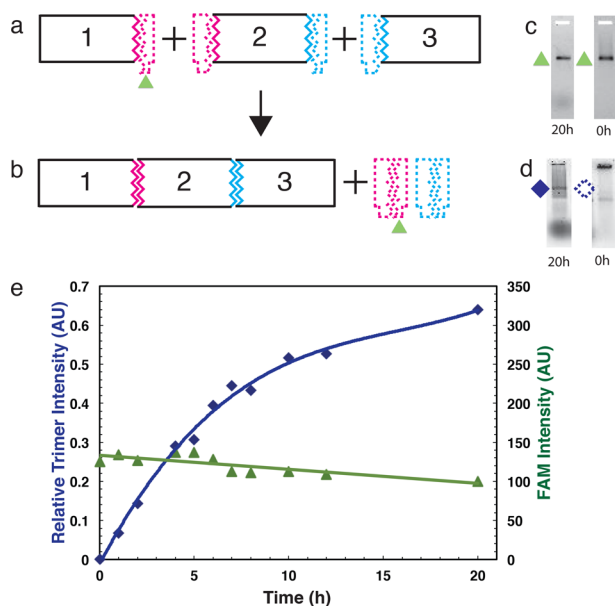


Figure 4. Time course assay to monitor displacement events with fluorescent labeling. (a) One protection tile (marked as a green triangle) in unit 1 was modified with a fluorophore (FAM) in the trimeric system. (b) Upon trimerization, the fluorescently labeled protection tile was displaced along with its partner from unit 2. (c) Agarose gel results with unit 1 alone (with FAM labeling) as a negative control (before SYBR gold poststaining). The fluorescent signal from FAM (green triangles) is stable over the 20 h time course. (d) Agarose gel results show the desired trimer (blue diamonds) formed gradually over the 20 h time course (after SYBR gold poststaining). (e) The blue curve shows the relative intensity of the trimer band against the monomer band upon SYBR gold poststaining. The green curve shows the fluorescent intensity (FAM) from unit 1 alone over the 20 h time course. Full results of the time course assay are in Figure S13.

however, it is difficult for SST structures to self-assemble properly when several single-stranded overhangs are present, as is the case for individual structural units with connection tiles at vertical boundaries.¹¹ Covering the single-stranded overhangs of the connection tiles with protection tiles before assembly mitigates this issue.

Covered sticky ends also lead to an energy normalization of individual complementation from sticky ends of different sequences to those from universal toeholds (T7/A7). Such a normalization eliminates the energy deviation by sticky ends of different sequences. Furthermore, we believe such a strand displacement process helps reduce undesired binding by random sticky end cohesion and hence preserves matching fidelity, since sticky ends are not exposed when higher-order assembly takes place. Because of the difficulty of preparing preformed SST units with exposed sticky ends, however, a direct comparison to show the enhanced assembly fidelity is not experimentally investigated.

Higher annealing temperature could encourage the combination of matching units, but the structural integrity could then be compromised if the temperature is too high. The protection tiles attached to the structure by a single 10/11nt domain are especially prone to fall off the structure at high temperature. Once the protection tiles fall off, the single-stranded overhangs from the connection tiles are exposed which encourages undesired random aggregation; however, the 10/11-nt domain generally provides stable enough binding at typical annealing

temperatures (e.g., 37 °C). If structural units with enhanced thermal stability are adopted (e.g., longer binding domains or enzymatic/chemical ligation to stitch multiple domains together),^{36,37} higher annealing temperatures could potentially be applied to increase the assembly yield of higher-order structures. With higher assembly fidelity, it is possible to construct more sophisticated DNA nanostructures (regular or irregular) with such an assembly method based on toehold-mediated strand displacement.

■ ASSOCIATED CONTENT

Supporting Information

The Supporting Information is available free of charge on the ACS Publications website at DOI: 10.1021/acs.nanolett.8b01355.

Designs and methods, additional results (AFM and agarose gel electrophoresis) and analysis, and DNA sequences (PDF)

■ AUTHOR INFORMATION

Corresponding Authors

*E-mail: bw@tsinghua.edu.cn.

*E-mail: py@hms.harvard.edu.

ORCID

Peng Yin: 0000-0002-2769-6357

Bryan Wei: 0000-0003-2515-2409

Present Addresses

#Bristol-Myers Squibb Company, Route 206 and Province Line Road, Princeton, NJ 08543, USA.

‡Department of Physics, Brandeis University, Waltham, MA 02453, USA.

△Janssen Research and Development, 1400 McKean Road, Spring House, PA 19477, USA.

Notes

The authors declare the following competing financial interest(s): Peng Yin is a cofounder of Ultivue Inc. and NuProbe Global.

■ ACKNOWLEDGMENTS

We thank Jeffrey Chen for technical assistance and David Zhang for helpful discussions. J.Y. acknowledges support from Tsinghua Xuetang Life Science Program. This work is supported by National Natural Science Foundation of China (31770926 and 31570860), “Thousand Talents Program” Young Investigator Award, funds from Beijing Advanced Innovation Center for Structural Biology, and a startup fund from the Tsinghua University-Peking University Joint Center for Life Sciences to B.W., University Grants Council of the Hong Kong Government Earmarked Grant (16302415) to Y.M. and B.W., Office of Naval Research (N00014-11-1-0914, N00014-13-1-0593, N00014-14-1-0610, and N00014-16-1-2182) and National Science Foundation (CCF-1054898, CCF-1162459, and CCF-1317291) to P.Y.

■ REFERENCES

- (1) Seeman, N. C. Nucleic-Acid Junctions and Lattices. *J. Theor. Biol.* **1982**, *99*, 237–247.
- (2) Fu, T. J.; Seeman, N. C. DNA Double-Crossover Molecules. *Biochemistry* **1993**, *32*, 3211–3220.
- (3) Winfree, E.; Liu, F. R.; Wenzler, L. A.; Seeman, N. C. Design and Self-Assembly of Two-Dimensional DNA Crystals. *Nature* **1998**, *394*, 539–544.

- (4) LaBean, T. H.; et al. Construction, Analysis, Ligation, and Self-Assembly of DNA Triple Crossover Complexes. *J. Am. Chem. Soc.* **2000**, *122*, 1848–1860.
- (5) Zhang, X. P.; Yan, H.; Shen, Z. Y.; Seeman, N. C. Paranemic Cohesion of Topologically-Closed DNA Molecules. *J. Am. Chem. Soc.* **2002**, *124*, 12940–12941.
- (6) Yan, H.; Park, S. H.; Finkelstein, G.; Reif, J. H.; LaBean, T. H. DNA-Templated Self-assembly of Protein Arrays and Highly Conductive Nanowires. *Science* **2003**, *301*, 1882–1884.
- (7) Shih, W. M.; Quispe, J. D.; Joyce, G. F. A. 1.7-Kilobase Single-Stranded DNA that Folds into a Nanoscale Octahedron. *Nature* **2004**, *427*, 618–621.
- (8) He, Y.; et al. Hierarchical Self-Assembly of DNA into Symmetric Supramolecular Polyhedra. *Nature* **2008**, *452*, 198–201.
- (9) Zheng, J. P.; et al. From Molecular to Macroscopic via the Rational Design of a Self-Assembled 3D DNA Crystal. *Nature* **2009**, *461*, 74–77.
- (10) Yin, P.; et al. Programming DNA Tube Circumferences. *Science* **2008**, *321*, 824–826.
- (11) Wei, B.; Dai, M. J.; Yin, P. Complex Shapes Self-Assembled from Single-Stranded DNA Tiles. *Nature* **2012**, *485*, 623–626.
- (12) Ke, Y. G.; Ong, L. L.; Shih, W. M.; Yin, P. Three-Dimensional Structures Self-Assembled from DNA Bricks. *Science* **2012**, *338*, 1177–1183.
- (13) Ong, L. L.; et al. Programmable Self-Assembly of Three-Dimensional Nanostructures from 10,000 Unique Components. *Nature* **2017**, *552*, 72–77.
- (14) Rothmund, P. W. K. Folding DNA to Create Nanoscale Shapes and Patterns. *Nature* **2006**, *440*, 297–302.
- (15) Dietz, H.; Douglas, S. M.; Shih, W. M. Folding DNA into Twisted and Curved Nanoscale Shapes. *Science* **2009**, *325*, 725–730.
- (16) Douglas, S. M.; et al. Self-Assembly of DNA into Nanoscale Three-Dimensional Shapes. *Nature* **2009**, *459*, 1154–1154.
- (17) Benson, E.; et al. DNA Rendering of Polyhedral Meshes at the Nanoscale. *Nature* **2015**, *523*, 441–444.
- (18) Zhang, F.; et al. Complex Wireframe DNA Origami Nanostructures with Multi-Arm Junction Vertices. *Nat. Nanotechnol.* **2015**, *10*, 779–784.
- (19) Veneziano, R.; et al. Designer Nanoscale DNA Assemblies Programmed from the Top Down. *Science* **2016**, *352*, 1534.
- (20) Iinuma, R.; et al. Polyhedra Self-Assembled from DNA Tripods and Characterized with 3D DNA-PAINT. *Science* **2014**, *344*, 65–69.
- (21) Marchi, A. N.; Saaem, I.; Vogen, B. N.; Brown, S.; LaBean, T. H. Toward Larger DNA Origami. *Nano Lett.* **2014**, *14*, 5740–5747.
- (22) Li, Z.; et al. Molecular Behavior of DNA Origami in Higher-Order Self-Assembly. *J. Am. Chem. Soc.* **2010**, *132*, 13545–13552.
- (23) Liu, W.; Zhong, H.; Wang, R.; Seeman, N. C. Crystalline Two-dimensional DNA-Origami Arrays. *Angew. Chem., Int. Ed.* **2011**, *50*, 264–267.
- (24) Rajendran, A.; Endo, M.; Katsuda, Y.; Hidaka, K.; Sugiyama, H. Programmed Two-Dimensional Self-Assembly of Multiple DNA Origami Jigsaw Pieces. *ACS Nano* **2011**, *5*, 665–671.
- (25) Tigges, T.; Heuser, T.; Tiwari, R.; Walther, A. 3D DNA Origami Cuboids as Monodisperse Patchy Nanoparticles for Switchable Hierarchical Self-Assembly. *Nano Lett.* **2016**, *16*, 7870–7874.
- (26) Tikhomirov, G.; Petersen, P.; Qian, L. Fractal Assembly of Micrometre-Scale DNA Origami Arrays with Arbitrary Patterns. *Nature* **2017**, *552*, 67–71.
- (27) Tikhomirov, G.; Petersen, P.; Qian, L. Programmable Disorder in Random DNA Tilings. *Nat. Nanotechnol.* **2017**, *12*, 251–259.
- (28) Woo, S.; Rothmund, P. W. Programmable Molecular Recognition Based on the Geometry of DNA Nanostructures. *Nat. Chem.* **2011**, *3*, 620–627.
- (29) Gerling, T.; Wagenbauer, K. F.; Neuner, A. M.; Dietz, H. Dynamic DNA Devices and Assemblies Formed by Shape-Complementary, Non-Base Pairing 3D Components. *Science* **2015**, *347*, 1446–1452.
- (30) Wagenbauer, K. F.; Sigl, C.; Dietz, H. Gigadalton-Scale Shape-Programmable DNA Assemblies. *Nature* **2017**, *552*, 78–83.
- (31) Suzuki, Y.; Endo, M.; Sugiyama, H. Lipid-Bilayer-Assisted Two-Dimensional Self-Assembly of DNA Origami Nanostructures. *Nat. Commun.* **2015**, *6*, 8052.
- (32) Zhao, Z.; Liu, Y.; Yan, H. Organizing DNA Origami Tiles into Larger Structures Using Preformed Scaffold Frames. *Nano Lett.* **2011**, *11*, 2997–3002.
- (33) Thompson, B. J.; Camien, M. N.; Warner, R. C. Kinetics of Branch Migration in Double-Stranded DNA. *Proc. Natl. Acad. Sci. U. S. A.* **1976**, *73*, 2299–2303.
- (34) Chen, S. X.; Zhang, D. Y.; Seelig, G. Conditionally Fluorescent Molecular Probes for Detecting Single Base Changes in Double-Stranded DNA. *Nat. Chem.* **2013**, *5*, 782–789.
- (35) Wei, B.; et al. Design Space for Complex DNA Structures. *J. Am. Chem. Soc.* **2013**, *135*, 18080–18088.
- (36) O'Neill, P.; Rothmund, P. W.; Kumar, A.; Fyngenson, D. K. Sturdier DNA Nanotubes via Ligation. *Nano Lett.* **2006**, *6*, 1379–1383.
- (37) Cassinelli, V.; et al. One-Step Formation of "Chain-Armor"-Stabilized DNA Nanostructures. *Angew. Chem., Int. Ed.* **2015**, *54*, 7795–7798.